SUB-MICRON PLASMONIC WAVEGUIDE FOR EFFICIENT SENSING OF BIO-FLUIDS

Rik Chattopadhyay, Rimlee D. Roy, and Shyamal K. Bhadra[*]

Fiber Optics and Photonics Division, CSIR-Central Glass and Ceramic Research Institute, 196, Raja S.C. Mullick Road, Jadavpur, Kolkata-700032, India

Abstract—A new sensor device is reported to measure the change in dielectric permittivity or refractive index of liquid samples. This novel device is extremely compact in nature and can be fabricated on a chip by integrated optical design method. The device works on change in surface plasmon (SP) amplitude to obtain permittivity values of samples adjacent to a specially designed metal-dielectric interface in a waveguide. The geometry of the interface has a distinct effect on sensitivity of measurement. The performance of the device is analyzed, and predicted through analytical and numerical calculations.

1. INTRODUCTION

Enhanced surface plasmon (SP) behavior at specially designed metal-dielectric interface would provide better refractive index sensing in planar waveguide structure [1, 2]. If the propagation constant of the incident light in dielectric medium is matched with that of the SP at metal-dielectric interface the surface plasmon polariton (SPP) mode is generated. This field penetrates a few hundred nanometers in the adjacent dielectric region, which is useful for detection of refractive index (RI) change in analyte. In a planar waveguide SP exists as a p-polarized (TM) wave when permittivity of the two adjacent media have opposite signs. Experimentally excitation of SP can be achieved by prism, grating and waveguide coupling methods [3–5]. In most cases SPR sensing are based on prism coupling of light as per Kretschmann configuration. These devices are bulk in size as they detect the change

of resonance reflectance angle with the variation in refractive index where the metal surface is exposed to sensing liquids [6, 7]. We propose a new method of sensing by observing the change in SP intensity resulting from change in permittivity. A planar waveguide with embedded metal layer probably the most robust and compact arrangement for sensitive detection.

In the present work we propose a scheme of SPP excitation that is based on the resonant transfer of incident photon energy from a guided and propagating core mode. The wave-vector matching condition for coupling the incident radiation to excite SPP is done through the index matching between different layers. In practical fabrication process a periodic relief pattern is embossed on the guiding medium using soft lithography technique and subsequently coated with silver of desired thickness in order to get efficient intensity of SPP. This way the change in the guided mode intensity along the direction of propagation is redistributed due to localization and the device becomes more sensitive to the change in permittivity or refractive index of analyte. Among other applications the process would help direct detection measurement of biomolecular interactions by monitoring either guided mode intensity or change in coupled SPP amplitude. A transverse magnetic (TM) polarized light beam from widely available He-Ne laser ($\lambda = 632.8\,\text{nm}$) is considered for the analysis. A comparative study of different geometry of metal-dielectric interfaces is also carried out through numerical simulation with LUMERICAL Mode Solution 5.0.3. to achieve best possible results. Later a miniaturized sensing device is proposed to monitor the behavior of biochemical fluids.

2. THEORETICAL MODELING

A schematic diagram of the waveguide structure is presented in Figure 1.

The waveguide is constructed with a substrate layer of index n_s, a guiding layer of index n_f and of thickness $d_f = 450\,\text{nm}$, a silver (Ag) layer of thickness $d_m = 30\,\text{nm}$ and index n_m and above the metal layer we introduce a cladding layer of index n_c. The interface of the guiding and metal layers has given a periodic perturbation similar to grating structure. The depth of the perturbation taken as $d_{grating} = 20\,\text{nm}$ and the period $\Lambda = 750\,\text{nm}$. All the dimensions have been achieved through an optimization and rigorous study of waveguide parameters so that only fundamental mode at operating wavelength of $632\,\text{nm}$ will be supported by the structure. We will try to show that the relief pattern in metal surface — indicated as the periodic perturbation would play an important role on guided core mode intensity.
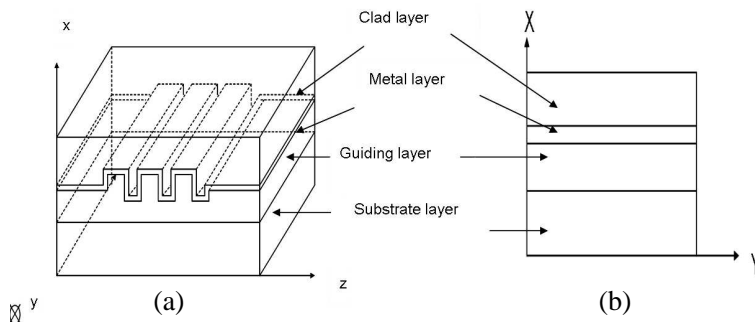
Figure 1. Schematic diagram of the waveguide with rectangular wall perturbation. (a) three dimensional view. (b) Transverse plane view.

We consider the light propagation along Z-axis and the waveguide is uniform and infinitely extended along Y-axis. The light propagation through this waveguide is modeled in two steps. First a modal analysis of the structure is done by removing the perturbation. Later the effect of perturbation on the desired propagating mode is studied for the index variation of analyte present adjacent to metal structure.

First we take the XY plane (Figure 1(b)). The waveguide becomes a simple four layer structure in this plane. Since we are interested to study plasmonic behavior we shall restrict our calculation for definite solution only for TM mode. We consider the input magnetic field as

$$
\begin{aligned}
H_y(x) &= A_1 \exp k_c(d_m - x) & \text{for } x \geq d_m \\
&= A_2 \cos(k_m x) + A_3 \sin(k_m x) & \text{for } d_m > x \geq 0 \\
&= A_4 \cos(k_f x) + A_5 \sin(k_f x) & \text{for } 0 > x \geq -d_f \\
&= A_6 \exp k_s(x + d_f) & \text{for } x < -d_f
\end{aligned}
\tag{1}
$$

where $k_s = \sqrt{(\beta^2 - k_0^2 \varepsilon_s)}$, $k_f = \sqrt{(k_0^2 \varepsilon_f - \beta^2)}$, $k_m = \sqrt{(k_0^2 \varepsilon_m - \beta^2)}$, $k_c = \sqrt{(\beta^2 - k_0^2 \varepsilon_c)}$, and β is the propagation constant of the desired mode and $k_0 = 2\pi/\lambda$ the free space wave vector at wavelength λ. $\varepsilon_i (= n_i^2)$ is the dielectric permittivity of the ith layer. A_1, A_2, A_3, A_4, A_5, A_6 are constants. Now we also have the relation between the electric field component and the magnetic field component in TM waveguide as

$$
E_z = -\frac{i}{n^2 \omega \varepsilon_0} \frac{\partial H_y}{\partial x}
\tag{2}
$$

Using the appropriate boundary conditions at the interfaces, i.e.,

$H_{1y} = H_{2y}$ and $\varepsilon_1 E_{1y} = \varepsilon_2 E_{2y}$ (since there is no free charge, i.e., $\sigma_f = 0$).

We get the following transcendental equation

$$\tan k_f d_f = \frac{-\frac{k_f}{n_f^2}A_5 + \frac{k_s}{n_s^2}A_4}{\frac{k_f}{n_f^2}A_5 + \frac{k_s}{n_s^2}A_4} \tag{3}$$

where the relation between A_5 and A_4 are given by the following relation

$$A_5 = A_4 \frac{\frac{k_m}{n_m^2}\sin k_m d_m - \frac{k_c}{n_c^2} \cos k_m d_m}{\frac{k_c k_f n_m^2}{k_m n_c^2 n_f^2}\sin k_m d_m + \frac{k_f}{n_f^2}\cos k_m d_m} \tag{4}$$

All other constants can be found out in terms of A_4 with the help of boundary conditions. We assume $A_4 = 1$. Using Equations (2), (3) and (4) we calculate the propagation constant β of the desired mode and effective index $n_{eff} = \beta/k_0$ of the desired mode. We choose the value of d_f in such a way that only the fundamental mode will propagate and other higher order modes leaked out. The refractive indices of subsequent layers are taken as $n_s = 1.453374$, $n_f = 1.7264$, $n_c = 1.33$ and $n_m = 0.0527369 + 4.2168656 * i$ at $\lambda = 632$ nm. Index of the silver is calculated by using Lorentz-Drude model [8]. We assume that the wall perturbation introduced in the waveguide will not change the modal profile, i.e., the transverse field distribution will not be affected by the perturbation [9]. In order to verify the assumption we analyzed the structure by FDTD and FEM mode solver (FDTD mode solver version 5.0.3 and also in Comsol multiphysics version 4.3a) at three different wavelengths with the perturbation. The geometry taken in FEM simulation is shown in Figure 1. Modal analysis of the structure is carried out to find out the effective index of the propagating fundamental mode and the results are compared with the analytical results, shown in Table 1. The results show a good match. Hence we can conclude that our preliminary assumption is correct, i.e., the perturbation does not affect the modal field distribution and modal propagation index.

Table 1. Effective index of the fundamental mode calculated through FDTD mode solver, analytical equation and Comsol Multiphysics 4.3a.

wavelength (nm)	n_{eff} (from FDTD mode solver)	n_{eff} (analytical values)	n_{eff} (from COMSOL multiphysics)
500	$1.656497 - i*6.966e-4$	$1.6471 - i*11.892e-4$	$1.647286 - i*11.99e-4$
632	$1.603546 - i*10.49084e-4$	$1.5882 - i*12.006e-4$	$1.588059 - i*12.14e-4$
850	$1.50544 - i*6.7796e-4$	$1.4876 - i*9.6592e-4$	$1.487124 - i*9.66e-4$

The difference between FDTD and analytically calculated values occurs as we have used values of silver index as provided in the FDTD software which are different from the values used in the analytical model. The analytical results showed a good match with the Comsol results. Yet we choose FDTD simulation as it is easier to find mode solution and propagation characteristics simultaneously for a complicated structure compare to (FEM simulation) Comsol. We choose the wavelength 632 nm as it is the output of the He-Ne laser and the structure is optimized at this wavelength to support the propagation of fundamental mode only. In Figure 2 we show the mode profile at 632 nm for three different clad indices, i.e., 1, 1.33 and 1.4. The results are compared with the results obtained from FDTD simulation.

From the Figures 2(a), (c), (e) it is clear that when the value of clad index increases the associated surface plasmon (SP) amplitude increases and simultaneously the intensity of the guided mode decreases as more and more power gets decoupled through SP. This change in SP amplitude can be explained through symmetric and asymmetric plasmon generation. The permittivities of the dielectric media adjacent to the metal layer, i.e., guiding layer and clad layer, are different. The guiding medium has high permittivity. When the permittivity of the clad layer (n_c) is low asymmetric SP is generated. When the permittivity of the clad is increased the asymmetric SP converts to symmetric SP, hence more power gets decoupled from the guiding layer through SP. This phenomenon can be used to convert this structure in sensor devices which will sense the change in refractive index or dielectric permittivity. Figures 2(b), (d), (f) show the results achieved through FDTD simulation. The results show that with an increment in clad index, the SP amplitude at metal clad interface increases. Modal analysis in XY plane is done using a propagator engine and a modal source with operating wavelength 632 nm with injection axis along Z. The mode profiles achieved through analytical solution and FDTD simulation are almost identical. Now we study the propagation characteristics of the structure. Using FDTD we studied the effect of the perturbation along the direction of propagation on this fundamental mode. The results are shown in Figure 3.

The mode profile remains intact through out the propagation but the amplitude varies in a periodic manner due to the perturbation present at the interface [9]. As evident the perturbation plays an important role in localizing the SP. The thickness of the guiding dielectric and metal layer varies periodically (Figure 1). This in turn changes the propagation constant of the guiding mode along direction of propagation and thus generates a backward propagating
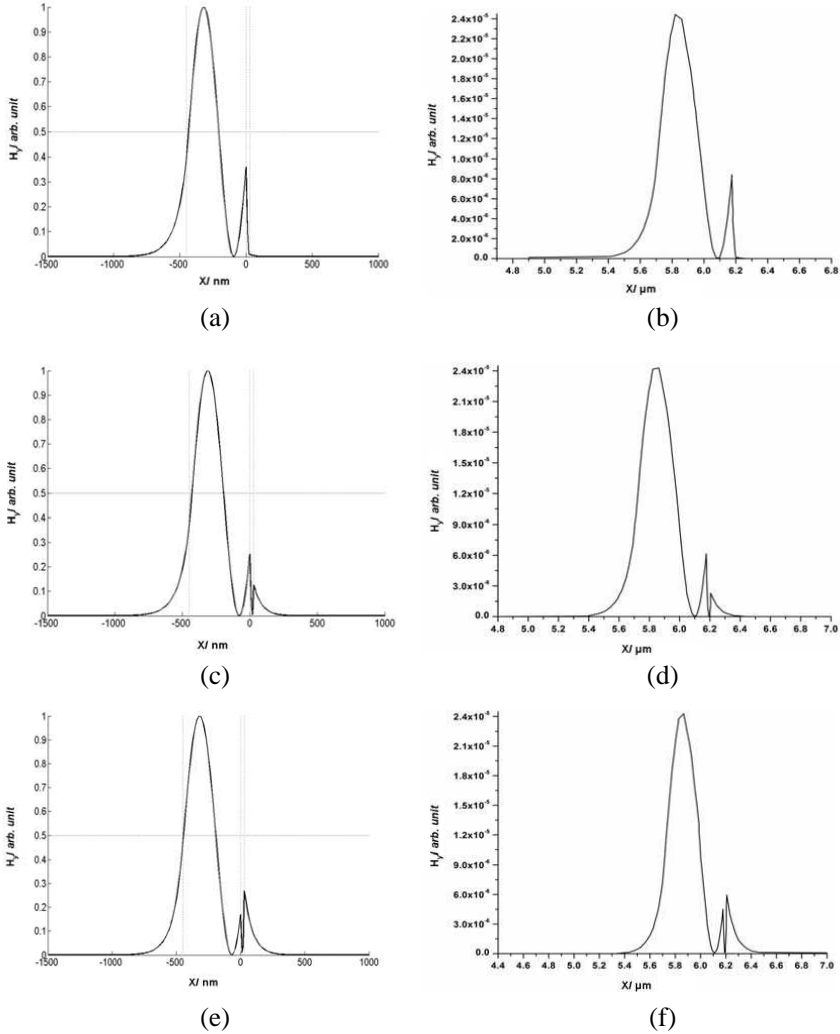
Figure 2. Transverse mode profile (H_y) from analytical calculation (a) $n_c = 1$, (c) $n_c = 1.33$, (e) $n_c = 1.4$, and (b), (d), (f) from FDTD mode solver for the same indices respectively.

mode [10]. The shape of the perturbation determines the amplitude variation of backward propagating wave. The superposition of the forward and backward wave localizes the SP by forming a standing wave pattern. FDTD simulation shows that SP modes are highly lossy, i.e., these modes are less propagating. It is well known that the
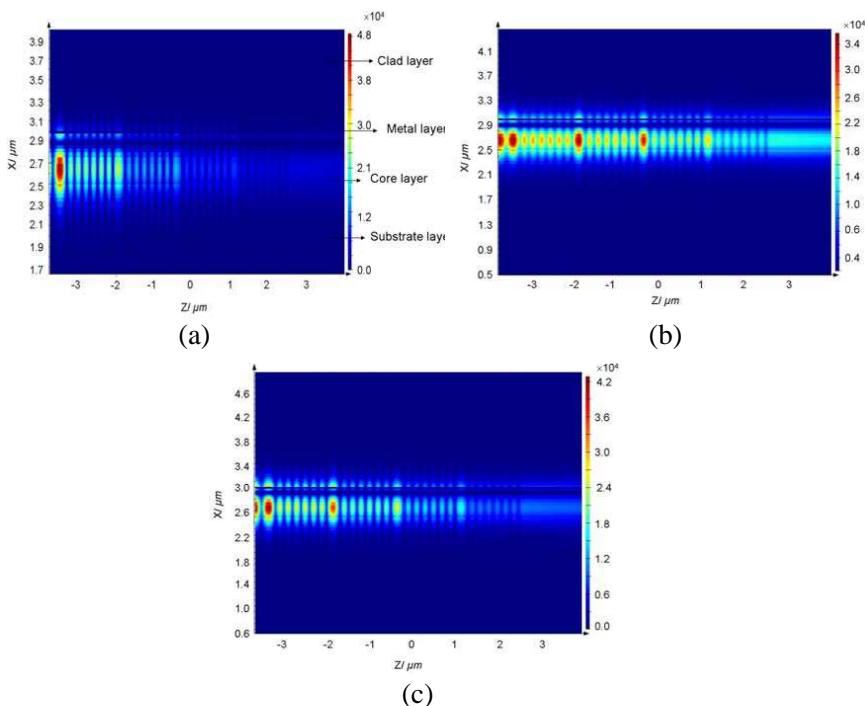
Figure 3. Propagation of the fundamental mode along Z axis and SP coupled mode for (a) $n_c = 1$, (b) $n_c = 1.33$, and (c) $n_c = 1.45$.

amplitude ratio of forward and backward propagating mode determines the amplitude of the antinodes. Therefore it is ensured that the profile of the perturbation would determine the amount of localized SP. The propagation distance also varies with the clad index. As a result the perturbation at the interface only localizes the SP and thus enhances the modal intensity to a certain distance. This would greatly help in measurement detection of index change in analyte.

After realizing the effect of the rectangular corrugation we now change the shape of the perturbation to understand its effect on propagating modes. It is well known that electric field intensity in tapered conductor gets concentrated at the tapered end. It is observed that SP accumulates strongly at sharp edges of metal dielectric interface [11–13]. It can be shown that the nonresonant SP enhancement at sharp tips occurs when the polarization of the incident light is parallel to the axis of the tip [14]. If we make the grating structure as shown in Figure 4, then the axis of the tip gets parallel
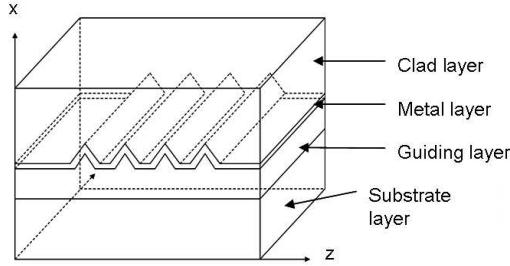
Figure 4. Schematic diagram of the waveguide with triangular wall perturbation with surface metal layer.

to the TM polarized field. So in this type of geometry maximum enhancement of SP at grating tips of triangular geometry is expected. Hence the change in perturbation to triangular geometry would give more intense localized SP. The schematic diagram is shown in Figure 4.

The propagation through this structure is also studied with the help of FDTD simulator. The results are shown in Figure 5 which show that SP localization is stronger and also the amplitude is higher than that of rectangular perturbation. The SP tends to accumulates at the tip of the triangles (Figure 4) and in turn it generates a strong back reflected SP. Hence the localization of SP increases as the forward and backward propagating SP modes have higher amplitudes.

Next we make a comparative study amongst — planar 4 layer waveguide without any perturbation, rectangular perturbation and triangular perturbation. The change in SP amplitude at the metal-guiding core layer interface is studied with variation of the clad index. The SP amplitude is taken after a propagation length of $5\,\mu$m at the metal-clad interface. The results are given in Figure 6. The SP amplitude is much higher in case of triangular geometry to the unperturbed or rectangular geometry at the interface. These results support our analytical prediction that triangular metallic-dielectric interface would be more sensitive for sensing variation of RI of analyte adjacent to metal surface.

According to our proposition we should get an opposite profile of SP amplitude at metal-guiding core layer interface if the clad index varied in similar fashion as shown in Figures 2(a), (c) & (e). We extended further the analytical calculation and the result is shown in Figure 7.

The analytical calculation shows that our proposition is right in the context that the amplitude of SP only depends on the structural parameters and indices of the layers. The perturbation does not

(a)

(b)

(c)
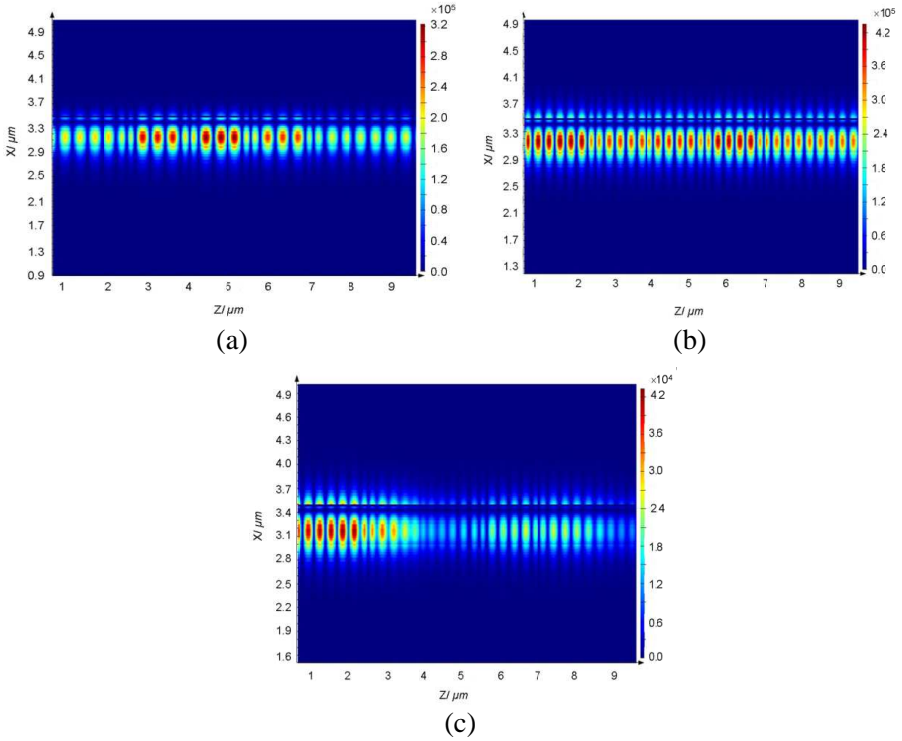
Figure 5. Propagation of the fundamental mode along Z axis. (a) $n_c = 1$. (b) $n_c = 1.33$. (c) $n_c = 1.45$.
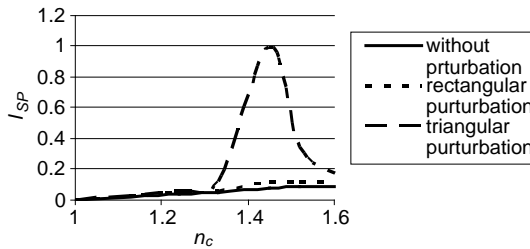
Figure 6. Variation of normalized SP amplitude (I_{SP}) at metal-clad interface with clad index (n_c) for different grating geometry at the interface.
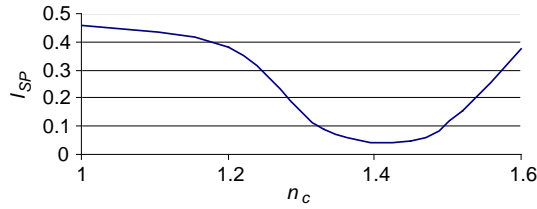
Figure 7. Variation of normalized SP amplitude (I_{SP}) with changing clad index (n_c) at metal-core interface.

changes the mode profile but only localizes the SP and thus makes the structure more sensitive to change in clad index.

3. PROPOSITION OF SENSING DEVICE

Based on the preceding observations we now propose a possible device configuration where the change in SP amplitude can be measured and in turn dielectric permittivity of different liquid or gas can be measured. The schematic diagram of the device is shown in Figure 8.
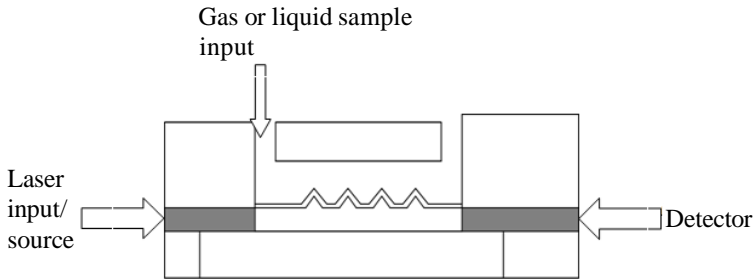
Figure 8. Schematic diagram of index sensing device.

As the gas or the liquid sample flows through the channel it will act as the clad material. If the output is calibrated then by measuring the change in output photo current different samples can be recognized or their dielectric permittivity can be determined. From Figure 6 we get that the change in SP amplitude is almost linear in the index region 1.4 to 1.6. This region can be used for measurement of dielectric permittivity. This device can be used to detect liquids such as Toluene, Benzene, Glycerin, Chloroform etc..

The most advantage of the device is that it can be implemented on a chip by using semiconductor laser (AlGaInP, AlGaAs) and photodetector.

4. CONCLUSION

The study shows that the sensitivity of the plasmonic device, in planar waveguide configuration, increases when a perturbation is introduced. It is also established that the shape profile of the perturbation at the interface of metallic-dielectric plays a significant role in increasing the detection sensitivity. The four layer configuration provides a compact and micro-arrangement for measuring the refractive index or permittivity which may not be possible with standard Kretschmann model. All existing angle or wavelength modulation based SPR sensor needs complicated and costly detection system to recognize the change in output signal. The proposed device needs a relatively simple opto-electronic circuit to measure the change in output. So it is cost effective and also an integrated device with embedded source and detector. This study only concentrates on two types of perturbation, i.e., rectangular and triangular, but with more varied structures the sensitivity can be enhanced much more. The linear range for measurement detection can be tailored by choosing different guiding core layers of optimized index profile. By changing the planar waveguide structure such as substrate and core layer one can tailor the operating region of the device. Similar sensing device can be developed using Au instead of Ag.

REFERENCES

1. Homola, J., S. S. Yee, and G. Gauglitz, "Surface plasmon resonance sensors: Review," *Sensors and Actuators B*, Vol. 54, Nos. 1–2, 3–15, 1999.
2. Nemova, G. and R. Kashyap, "Theoretical model of a planar integrated refractive index sensor based on surface plasmon-polariton excitation with a long period garting," *J. Opt. Soc. Am. B*, Vol. 24, No. 10, 2696, 2007.
3. Hong, S. H., C. K. Kong, B. S. Kim, M. W. Lee, S. G. Lee, S. G. Park, E. H. Lee, and O. Beom-Hoan, "Implementation of surface plasmon resonance planar waveguide sensor system," *Microelectron. Eng.*, Vol. 87, 1315, 2010.

4. Luo, Z., T. Suyama, X. Xu, and Y. Okuno, "A grating-based plasmon biosensor with high resolution," *Progress In Electromagnetics Research*, Vol. 118, 527–539, 2011.

5. Guillod, T., F. Kehl, and C. Hafner, "FEM-based method for the simulation of dielectric waveguide grating biosensors," *Progress In Electromagnetics Research*, Vol. 137, 565–583, 2013.

6. Homola, J., J. Ctyroky, M. Skalsky, J. Hradilova, and P. Kolarova, "A surface plasmon resonance based integrated optical sensor," *Sens. Act. B*, Vol. 286, 38–39, 1997.

7. Liedberg, B., C. Nylander, and I. Lundstrom, "Surface plasmon resonance for gas detection and biosensing," *Sens. Act.*, Vol. 4, 299, 1983.

8. Rakić, A. D., A. B. Djurišić, J. M. Elazar, and M. L. Majewski, "Optical properties of metallic films for vertical-cavity optoelectronic devices," *App. Opt.*, Vol. 37, No. 22, 5271–5283, 1998.

9. Homola, J. and O. S. Wolfbeis, "Surface plasmon resonance based sensors," *Springer Series on Chemical Sensors and Biosensors*, Vol. 4, Part 1, Chapter 3, Springer-Verlag Berlin Heidelberg, 2006.

10. Min, C. and G. Veronis, "Theoretical investigation of fabrication-related disorders on the properties of subwavelength metal-dielectric-metal plasmonic waveguides," *Optics Express*, Vol. 18, 20939, Aug. 2010.

11. Maier, S. A. and H. A. Atwater, "Plasmonics: Localization and guiding of electromagnetic energy in metal/dielectric structures," *Journal of Applied Physics*, Vol. 98, 011101, 2005.

12. Kauranen, M. and A. V. Zayats, "Nonlinear plasmonics," *Nature Photonics*, Vol. 6, 737, Nov. 2012.

13. Lal, S., S. Link, and N. J. Halas, "Nano-optics from sensing to waveguiding," *Nature Photonics*, Vol. 1, 641, Nov. 2007.

14. Stockman, M. I., "Nanoplasmonics: The physics behind the application," *Physics Today*, 39–44, Feb. 2011.